Sensitivity and Validation Studies of Plutonium-238 Production with Shift and ORIGEN[1]

D. Chandler,* D. Hartanto, J. W. Bae, K. M. Burg, and Y. E. Robert

*Oak Ridge National Laboratory, P.O. Box 2008, Oak Ridge, TN 37831-6170, USA, *chandlerd@ornl.gov*

INTRODUCTION

This paper presents results from a series of ^{238}Pu production sensitivity and validation studies to support the ^{238}Pu Supply Project (PSP) and the conversion of the High Flux Isotope Reactor (HFIR) from highly enriched uranium (HEU) fuel to low-enriched uranium (LEU) fuel. In support of the PSP, HFIR produces ^{238}Pu to be used as a power source for NASA. Additionally, HFIR's mission capabilities must be maintained or enhanced after LEU conversion to sustain the facility's world-leading scientific capabilities. Thus, it is vital to characterize ^{238}Pu production to support ongoing PSP activities and to define baseline metrics for future comparisons with proposed LEU fuel designs. The SCALE Shift and ORIGEN [1,2] codes are used to characterize ^{238}Pu production metrics with the current HEU-fueled core based on a recent irradiation campaign.

High Flux Isotope Reactor

HFIR is an 85 MW thermal, HEU-fueled (U_3O_8-Al, ~93 wt %), pressurized, light-water–cooled and –moderated, beryllium-reflected research reactor operated at Oak Ridge National Laboratory (ORNL) on behalf of the US Department of Energy (DOE) Office of Science (SC). The core design consists of a central flux trap nested inside two fuel elements which are surrounded by two concentric control elements and a large beryllium reflector (Fig. 1).

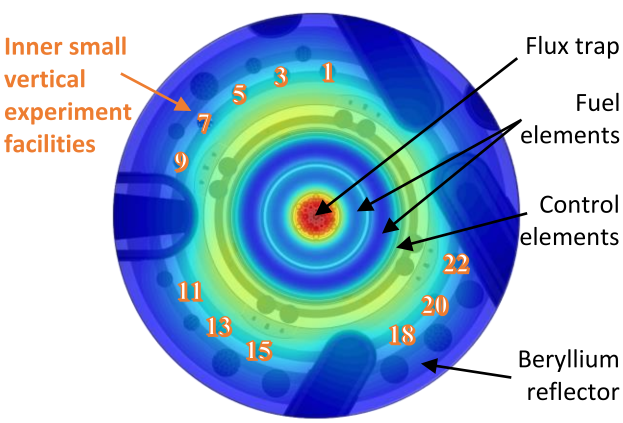

Fig. 1. HFIR core model and thermal flux distribution.

HFIR was designed with a compact high-power density core to promote neutron leakage into experiment regions, thus enabling unparalleled in-vessel irradiation facility flux environments. HFIR is used for neutron scattering research, isotope production, materials and fuels irradiation research, neutron activation analysis, and other radiation-based research. Refer to the article by Chandler et al. [3] for more details on the core design, operations, and missions.

Plutonium-238 Supply Project

The purpose of the ORNL-led PSP is to establish a domestic supply of ^{238}Pu produced in HFIR and the Advanced Test Reactor at Idaho National Laboratory [4]. Radioisotope power systems are fueled with PuO_2 pellets and convert ^{238}Pu decay heat into electrical power for NASA deep-space and planetary missions such as the Perseverance rover on Mars. Irradiation of ^{237}Np-bearing targets in HFIR's beryllium reflector vertical experiment facilities (VXFs) results in efficient production of ^{238}Pu. ^{238}Pu is produced via neutron capture in ^{237}Np and subsequent beta decay of ^{238}Np (2.12 day half-life). Sensitivity and validation studies are performed to improve production yield predictions, better understand production sensitivities, and provide confidence in codes and data being used to continuously design and qualify targets for improved production and safety.

Low-Enriched Uranium Conversion

HFIR is evaluating conversion to LEU fuel as part of the DOE National Nuclear Security Administration (NNSA) Office of Material Management and Minimization (M3) mission to eliminate the use of HEU in civilian nuclear applications to the greatest extent possible. Several LEU U_3Si_2-Al designs have been documented that meet key performance metrics (KPMs) such as thermal fluxes to selected irradiation facilities if power is increased from 85 to 95 MW [5,6]. An LEU-fueled core must maintain or exceed the HEU core KPMs to be considered a candidate. Ongoing higher fidelity modeling and simulation (M&S) studies such as those documented herein will provide additional confidence that a 95 MW LEU core can maintain 85 MW HEU-like performance.

STUDY TOOLS AND DATA

Version 7.0 Beta 7 of the SCALE nuclear M&S software was used for this effort. The computationally efficient Shift Monte Carlo–based transport and depletion tool with ORIGEN was deployed for neutron transport, fuel depletion (418 materials), control element withdrawal and activation (80 materials), and ^{238}Pu production calculations. The HEU core input with simplified fuel and representative experiment loading models [3] was used as the basis for these studies. Continuous-energy cross sections based on ENDF/B-VII.1 libraries were used [7]. Each transport step simulated 100 million active histories and 5 million inactive histories. Tallies were defined in the depletion calculations to characterize intracycle fluxes and fission rate densities for each ^{238}Pu production target cell. Standalone ORIGEN calculations were performed for follow-on production, sensitivity coefficient analysis, and other parametric studies.

TARGET AND IRRADIATION DATA

Campaign 6 consisted of 63 generation II full-length production targets irradiated during cycles 486 (January 2020 start) and 487 (May 2020 end). Cycle 486 operated for 2,126.02 MWd (25.01 days at 85 MW), and cycle 487 operated for 2,136.99 MWd (25.14 days at 85 MW). Control element withdrawal curves from these cycles were used in the depletion calculations. Generation II targets consist of a stack of 52 NpO_2/Al pellets loaded in an Al cladding tube. The pellets are nominally composed of 20 vol % NpO_2, 70 vol % Al, and 10 vol % void. The pellets are approximately 0.32 cm in radius and 0.96 cm in length. Seven targets are loaded into an assembly which is loaded into a small VXF. The assembly is arranged such that one of the six peripheral targets directly faces the core. One target is centrally loaded in the assembly. Targets were loaded in VXFs 1, 3, 5, 11, 13, 15, 18, 20, and 22. The total ^{238}Pu recovered from campaign 6 was 166.39 g (2.64 g/target). A minimum conservatively assumed recovery fraction of 0.95 results in a maximum possible production of approximately 175.15 g (2.78 g/target).

CALCULATIONAL RESULTS

A systematic progression of sensitivity and validation studies assessing impacts of the modeled temporal mesh, spatial mesh, temperature, reaction data, and flux on ^{238}Pu production is described in the following sections.

Shift Temporal Mesh Sensitivity Study

Multi-cycle experiment depletion studies are time consuming, so a temporal mesh sensitivity study was performed to determine the impact of time resolution on ^{238}Pu production. Five cases simulating 25, 19, 16, 13, and 10 depletion steps throughout each of the ~25 day irradiation cycles were executed, and the step sizes were determined based on the movement of the control elements. One-day time steps were simulated near the beginning and end of each cycle for all cases. Each of the 63 NpO_2/Al pellet stacks was modeled as a single cylinder based on the as-built pellet stack length, radius, and NpO_2 loading. Figure 2 illustrates the k_{eff} curves for the five cases and shows good agreement throughout the cycles. Excess reactivity is calculated at beginning-of-cycle, which is assumed to be due to modeling fresh control element and beryllium reflector materials.

Production results are compared in Fig. 3 and Table I. The calculated ^{238}Pu masses vary between 180.41 and 180.90 g (2.86–2.87 g/target), which are ~3–9% greater than the measured mass (assuming 95–100% recovery). The temporal mesh has little impact on ^{238}Pu production and quality (i.e., ^{238}Pu to total Pu ratio); however, the number of time steps and run times are linearly related, as expected. Smaller time steps do capture some other metrics a little better such as fission rate densities and ^{236}Pu production. All five temporal meshes are deemed appropriate for this study; however, the 16 depletion–step temporal mesh is preferred to balance run time and temporal fidelity.

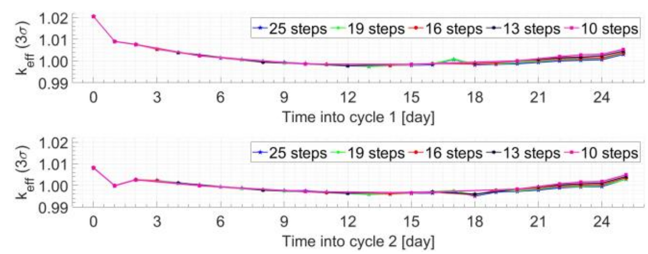

Fig. 2. Effective multiplication curves.

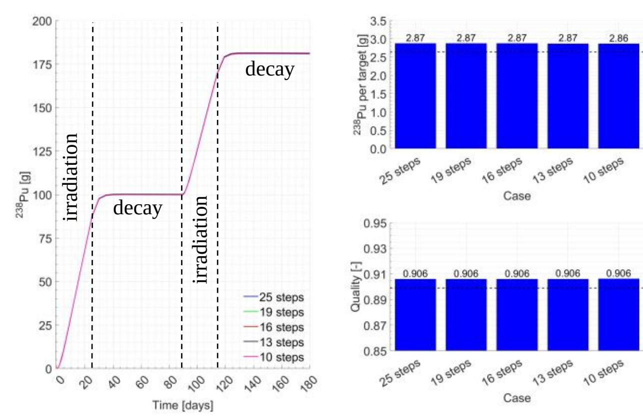

Fig. 3. ^{238}Pu production and quality for time-step cases.

TABLE I. Temporal mesh study summary

Case	^{238}Pu		Run Time
	[g-Total]	[g/Target]	[CPU-Day]
10 steps	180.90	2.87	90
13 steps	180.84	2.87	110
16 steps	180.74	2.87	134
19 steps	180.65	2.87	159
25 steps	180.41	2.86	208

Shift Spatial Mesh Sensitivity Study

The spatial mesh can be important for capturing self-shielding effects and for calculating local results such as fission and heating rates. To characterize the impact of the modeled spatial mesh, 27 unique meshes were modeled in three Shift cases. The three cases modeled 7, 9, and 11 axial zones per stack of NpO_2/Al pellets. The pellet stacks within each VXF had a unique radial-by-azimuthal mesh, as shown in Fig. 4 (red arrows point to core centerline). A 3-radial by 3-azimuthal matrix was evaluated for each case, including 1, 2, or 3 radial zones and 2, 4, or 6 azimuthal zones. Evaluating 9 different meshes in each case reduces total Shift cases from 27 to 3, thereby significantly reducing computational resource requirements. The 16 depletion–step temporal mesh case was utilized as the reference case for this study.

Figure 5 and Table II summarize the spatial mesh results. Consideration of finer spatial meshes has a small impact on calculated ^{238}Pu production, perhaps, less than expected. The case modeling 5,544 NpO_2/Al cells predicted approximately 1% less ^{238}Pu and took approximately 13% more computational time relative to the reference case only modeling 63 NpO_2/Al cells. Figure 5 illustrates the ratio of spatial mesh results to those of the reference case. None of the higher resolution meshes resulted in greater than a 1% change relative to the reference case.

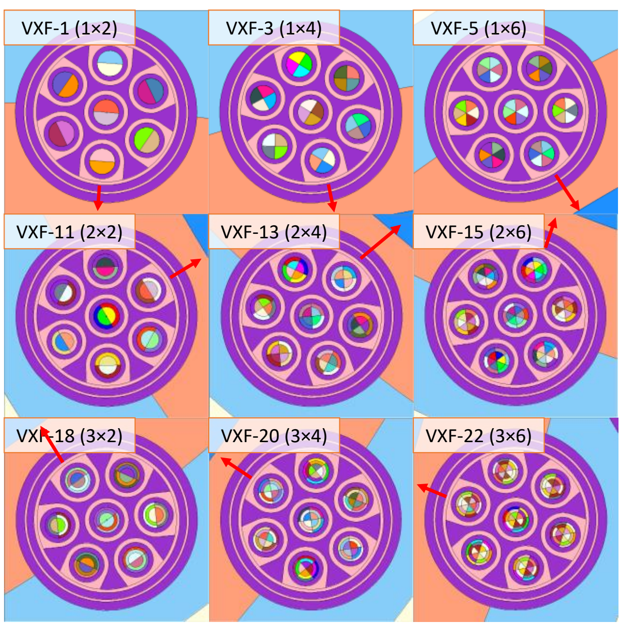

Fig. 4. Radial-by-azimuthal (R × A) mesh discretization.

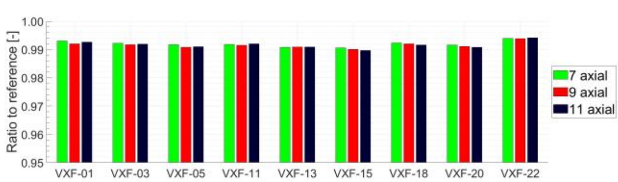

Fig. 5. Impact of spatial mesh on ^{238}Pu production.

TABLE II. Spatial mesh study summary

Case	NpO_2/Al Cells	^{238}Pu [g/Target]	Run Time [CPU-Day]
Reference	63	2.87	134
7 axial	3,528	2.85	142
9 axial	4,536	2.84	149
11 axial	5,544	2.84	152

Shift Temperature Sensitivity Study

Pellet heat deposition rates change throughout irradiation mostly because of the generation of the fissile ^{238}Np and ^{239}Pu isotopes [4]. Furthermore, densification and swelling changes the gas gap distance between pellets and cladding, so temperatures vary in both time and space. A temperature sensitivity study was performed to determine the impact of temperature on ^{238}Pu production.

The 16-step temporal mesh case with 63 NpO_2/Al cells at 293.6 K was used as the reference case. The materials in each VXF were changed between 400 and 1,200 K in 100 K increments. Figure 6 illustrates the ratio of temperature perturbation results to those of the reference case. Production slightly increases as temperature increases, but the increases only vary between 0.0 and 0.7%, so production is not very sensitive to target temperature assumptions.

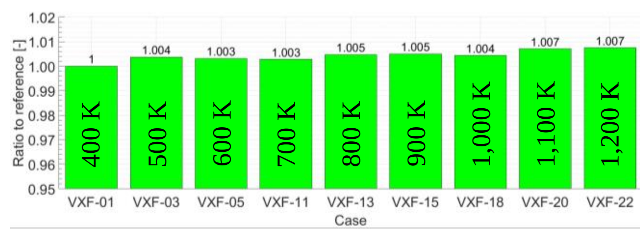

Fig. 6. Impact of temperature on ^{238}Pu production.

ORIGEN Sensitivity Coefficient Study

ORIGEN was used to calculate the sensitivity coefficients using adjoint-based depletion perturbation theory to better understand the reaction and decay channels important to ^{238}Pu production. The time- and space-averaged 252-energy group flux, total flux ($3.52 \times 10^{+14}$ n/cm^2·s), and one-group cross sections were computed from the Shift 25 depletion–step case and input to ORIGEN. The resultant ^{238}Pu production was 182.30 g (2.89 g/target), which is within 1% of the Shift calculations and 10% of the measurement.

The pertinent reaction cross sections, decay constants, and sensitivity coefficients are provided in Table III. The sensitivity coefficients are expressed as the relative change in ^{238}Pu production per change in the reaction channel, and the greatest coefficient is for ^{237}Np(n,γ). ^{238}Pu production increases 0.94% if the ^{237}Np(n,γ) cross section increases by 1.00%. Notable sensitivity coefficients were also calculated for ^{238}Np β^- decay, ^{238}Np(n,f), and ^{238}Pu(n,γ).

TABLE III. ^{238}Pu Production Sensitivity Coefficients

Nuclide	Reaction	Cross Section or Decay Constant	Sensitivity Coefficient
^{237}Np	*(n,γ)*	$7.96 \times 10^{+01}$ b	$+9.38 \times 10^{-01}$
	(n,f)	1.93×10^{-01} b	-1.51×10^{-04}
^{238}Np	β^- decay	3.78×10^{-06} s^{-1}	$+6.26 \times 10^{-02}$
	(n,γ)	$1.85 \times 10^{+02}$ b	-1.40×10^{-03}
	(n,f)	$9.33 \times 10^{+02}$ b	-7.06×10^{-02}
^{238}Pu	α decay	2.50×10^{-10} s^{-1}	-4.65×10^{-03}
	(n,γ)	$1.47 \times 10^{+02}$ b	-9.84×10^{-02}
	(n,f)	$6.95 \times 10^{+00}$ b	-4.66×10^{-02}

ORIGEN Flux Sensitivity Study

A parametric study was carried out using the Sampler uncertainty analysis tool to uniformly vary the time- and space-averaged total flux from 3.0×10^{14} to 4.0×10^{14} n/cm^2·s. The ORIGEN input discussed in the sensitivity coefficient section was modified for use with Sampler. The resultant ^{238}Pu production variation with total flux curve is provided in Fig. 7. The Shift-calculated total flux of $3.52 \times 10^{+14}$ n/cm^2·s may be overestimated by approximately 5–11% based on comparison with total fluxes required to obtain ^{238}Pu masses corresponding to the 95 and 100% material recovery assumptions.

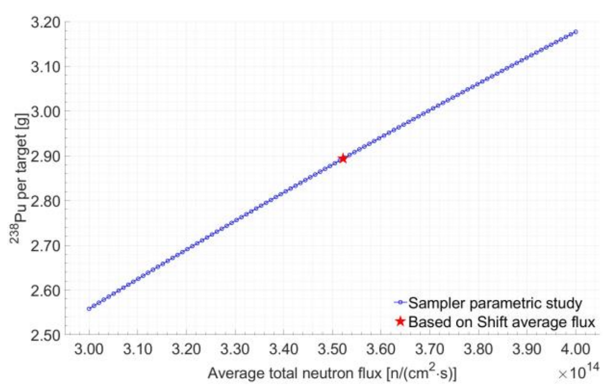

Fig. 7. ^{238}Pu production variation with flux.

CONCLUSIONS AND FUTURE WORK

Detailed ^{238}Pu production sensitivity and validation studies were performed in support of HFIR's goals to produce ^{238}Pu efficiently and reliably and to maintain performance with a future LEU core. A systematic progression of sensitivity studies assessing impacts of the modeled temporal mesh, spatial mesh, temperature, data, and flux on ^{238}Pu production was executed with the Shift and ORIGEN codes. ^{238}Pu production is not strongly correlated to the temporal meshes, spatial meshes, or temperatures considered in this study. However, ^{238}Pu production is sensitive to flux changes and nuclear data such as the ^{237}Np*(n,γ)* cross section. Calculations are overpredicting production by approximately 2–9% based on results from a recent irradiation campaign.

The next steps in this work include consideration of as-irradiated materials surrounding the targets, other data libraries (e.g., ENDF/B-VIII), and other depletion tools (e.g., HFIRCON). Modeling as-irradiated control element and beryllium reflector materials is expected to reduce the targets' flux (and core excess reactivity), thereby better aligning the results and measurements. Similar studies will then be performed with a proposed LEU core. A ^{238}Pu production comparison with an LEU core should provide additional confidence that an LEU core can maintain HFIR's ability to produce the critically important ^{238}Pu isotope.

ACKNOWLEDGMENTS

This research was performed on HFIR, a DOE-SC User Facility operated by ORNL under contract DE-AC05-00OR22725. This research was supported by DOE NNSA's Office of M3, NASA's Science Mission Directorate, and DOE's Office of Nuclear Infrastructure Programs. The author's thank C. Jensen and D. DePaoli for providing the as-built target data and the campaign measurement data, respectively. The authors acknowledge C. Sizemore, ORNL LEU conversion manager, and A. Parkison, ORNL PSP manager, for their support. The author's thank T. Greene, A. Holzaepfel, and Z. Karriem for their reviews of this paper.

REFERENCES

1. W. WIESELQUIST and R. LEFEBVRE, Eds., *SCALE 6.3.1 User Manual*, ORNL/TM-SCALE-6.3.1 (2023).
2. T. PANDYA, S. JOHNSON, T. EVANS, et al., "Implementation, Capabilities, and Benchmarking of Shift, a Massively Parallel Monte Carlo Radiation Transport Code." *J. Comp. Phys.* **308**, 239–272 (2016).
3. D. CHANDLER, B. BETZLER, E. DAVIDSON, and G. ILAS, "Modeling and Simulation of a High Flux Isotope Reactor Representative Core Model for Updated Performance and Safety Basis Assessments," *Nucl. Eng. Des.*, **366**, 110752 (2020).
4. D. CHANDLER and C. DAILY, "Deployment of the HFIRCON Transport and Depletion Tool for Plutonium-238 Production Studies," *Proc. PHYSOR 2022*, 1913–1922 (2022).
5. J. BAE, B. BETZLER, D. CHANDLER, G. ILAS, and J. MESZAROS, *High Flux Isotope Reactor Low Enriched Uranium High Density Silicide Fuel Design Parameters*, ORNL/TM-2020/1799 (2021).
6. B. BETZLER, D. CHANDLER, J. BAE, G. ILAS, and J. MESZAROS, *High Flux Isotope Reactor Low Enriched Uranium Low Density Silicide Fuel Design Parameters*, ORNL/TM-2020/1798 (2021).
7. M.B. CHADWICK, et al., "ENDF/B-VII.1 Nuclear Data for Science and Technology: Cross Sections, Covariances, Fission Product Yields and Decay Data," *Nuclear Data Sheets*, **112**, 2887–2996 (2011).